HYPERGRAPH PARTITIONING BASED MODELS AND METHODS FOR EXPLOITING CACHE LOCALITY IN SPARSE MATRIX-VECTOR MULTIPLICATION*

KADIR AKBUDAK†, ENVER KAYAASLAN†, AND CEVDET AYKANAT†

Abstract. Sparse matrix-vector multiplication (SpMxV) is a kernel operation widely used in iterative linear solvers. The same sparse matrix is multiplied by a dense vector repeatedly in these solvers. Matrices with irregular sparsity patterns make it difficult to utilize cache locality effectively in SpMxV computations. In this work, we investigate single- and multiple-SpMxV frameworks for exploiting cache locality in SpMxV computations. For the single-SpMxV framework, we propose two cache-size–aware row/column reordering methods based on one-dimensional (1D) and two-dimensional (2D) top-down sparse matrix partitioning. We utilize the column-net hypergraph model for the 1D method and enhance the row-column-net hypergraph model for the 2D method. The primary aim in both of the proposed methods is to maximize the exploitation of temporal locality in accessing input vector entries. The multiple-SpMxV framework depends on splitting a given matrix into a sum of multiple nonzero-disjoint matrices. We propose a cache-size–aware splitting method based on 2D top-down sparse matrix partitioning by utilizing the row-column-net hypergraph model. The aim in this proposed method is to maximize the exploitation of temporal locality in accessing both input- and output-vector entries. We evaluate the validity of our models and methods on a wide range of sparse matrices using both cache-miss simulations and actual runs by using OSKI. Experimental results show that proposed methods and models outperform state-of-the-art schemes.

Key words. cache locality, sparse matrix, matrix-vector multiplication, matrix reordering, computational hypergraph model, hypergraph partitioning, traveling salesman problem

AMS subject classifications. 65F10, 65F50, 65Y20

DOI. 10.1137/100813956

1. Introduction. Sparse matrix-vector multiplication (SpMxV) is an important kernel operation in iterative linear solvers used for the solution of large, sparse, linear systems of equations. In these iterative solvers, the SpMxV operation $y \leftarrow Ax$ is repeatedly performed with the same large, irregularly sparse matrix A. Irregular access patterns during these repeated SpMxV operations cause poor usage of CPU caches in today's deep memory hierarchy technology. However, SpMxV operations can possibly exhibit very high performance gains if temporal and spatial localities are respected and exploited properly. Here, temporal locality refers to the reuse of data words (e.g., x-vector entries) before eviction of the words from cache, whereas spatial locality refers to the use of data words (e.g., matrix nonzeros) within relatively close storage locations (e.g., in the same lines) in the very near future. In this work, the main motivation is our expectation that exploiting temporal locality is more important than exploiting spatial locality (for practical line sizes) in SpMxV operations that involve irregularly sparse matrices.

In this work, we investigate two distinct frameworks for the SpMxV operation: single-SpMxV and multiple-SpMxV frameworks. In the single-SpMxV framework, the y-vector results are computed by performing a single SpMxV operation $y \leftarrow Ax$.

In the multiple-SpMxV framework, the $y \leftarrow Ax$ operation is computed as a sequence of multiple input- and output-dependent SpMxV operations, $y \leftarrow y + A^k x$ for $k = 1, \ldots, K$, where $A = A^1 + \cdots + A^K$.

For the single-SpMxV framework, we propose two cache-size–aware row/column reordering methods based on top-down one-dimensional (1D) and two-dimensional (2D) partitioning of a given sparse matrix. The primary objective in both methods is to maximize the exploitation of temporal locality in accessing x-vector entries, whereas the exploitation of spatial locality in accessing x-vector entries is a secondary objective. The 1D partitioning based method relies on transforming a sparse matrix into a singly bordered block-diagonal (SB) form by utilizing the column-net hypergraph model given in [4, 7, 8]. The 2D partitioning based method relies on transforming a sparse matrix into a doubly bordered block-diagonal (DB) form by utilizing the row-column-net hypergraph model given in [11, 10]. We provide upper bounds on the number of cache misses based on these transformations and show that the objectives in the transformations based on partitioning the respective hypergraph models correspond to minimizing these upper bounds. In the 1D partitioning based method, the column-net hypergraph model correctly encapsulates the minimization of the respective upper bound. For the 2D partitioning based method, we propose an enhancement to the row-column-net hypergraph model to encapsulate the minimization of the respective upper bound on the number of cache misses.

For the multiple-SpMxV framework, we propose a matrix splitting method that tries to maximize the exploitation of temporal locality in accessing both x-vector and y-vector entries during individual $y \leftarrow y + A^k x$ computations. In the proposed method, we use a cache-size–aware top-down approach based on 2D sparse matrix partitioning by utilizing the row-column-net hypergraph model given in [11, 10]. We provide an upper bound on the number of cache misses based on this matrix splitting and show that the objective in the hypergraph partitioning (HP) based matrix partitioning exactly corresponds to minimizing this upper bound. For this framework, we also propose two methods for effective ordering of individual SpMxV operations.

We evaluate the validity of our models and methods on a wide range of sparse matrices. The experiments are carried out in two different settings: cache-miss simulations and actual runs by using OSKI (BeBOP Optimized Sparse Kernel Interface Library) [39]. Experimental results show that the proposed methods and models outperform state-of-the-art schemes, and these results also conform to our expectation that temporal locality is more important than spatial locality (for practical line sizes) in SpMxV operations that involve irregularly sparse matrices.

The rest of the paper is organized as follows: Background material is introduced in section 2. In section 3, we review some of the previous works about iteration/data reordering and matrix transformations for exploiting locality. The two frameworks along with our contributed models and methods are described in section 4. We present the experimental results in section 5. Finally, the paper is concluded in section 6.

2. Background.

2.1. Sparse-matrix storage schemes. There are two standard sparse-matrix storage schemes for the SpMxV operation: *compressed storage by rows* (CSR) and *compressed storage by columns* (CSC) [5, 33]. Without loss of generality, in this paper, we restrict our focus to the conventional SpMxV operation using the CSR storage scheme, whereas cache-aware techniques such as prefetching and blocking are outside the scope of this paper. In the following paragraphs, we review the standard CSR scheme and two CSR variants.

The CSR scheme contains three 1D arrays: *nonzero*, *colIndex*, and *rowStart*. The values and the column indices of nonzeros are, respectively, stored in row-major order in the *nonzero* and *colIndex* arrays in a one-to-one manner. The *rowStart* array stores the index of the first nonzero of each row in the *nonzero* and *colIndex* arrays.

The *zig-zag CSR* (ZZCSR) scheme was proposed to reduce end-of-row cache misses [41]. In ZZCSR, nonzeros are stored in increasing column-index order in even-numbered rows, whereas they are stored in decreasing index order in odd-numbered rows, or vice versa.

The *incremental compressed storage by rows* (ICSR) scheme [27] is reported to decrease instruction overhead by using pointer arithmetic. In ICSR, the *colIndex* array is replaced with the *colDiff* array, which stores the increments in the column indices of the successive nonzeros stored in the nonzero array. The *rowStart* array is replaced with the *rowJump* array, which stores the increments in the row indices of the successive nonzero rows. The ICSR scheme has the advantage of handling zero rows efficiently since it avoids the use of the *rowStart* array. This feature of ICSR is exploited in our multiple-SpMxV framework since this scheme introduces many zero rows in the individual sparse matrices. Details of the SpMxV algorithms utilizing CSR and ICSR are described in our technical report [2].

2.2. Data locality in CSR-based SpMxV. In accessing matrix nonzeros, temporal locality is not feasible since the elements of each of the *nonzero*, *colIndex* (*colDiff* in ICSR), and *rowStart* (*rowJump* in ICSR) arrays are accessed only once. Spatial locality is feasible, and it is achieved automatically by nature of the CSR scheme since the elements of each of these three arrays are accessed consecutively.

In accessing y-vector entries, temporal locality is not feasible since each y-vector result is written only once to the memory. From a different point of view, temporal locality can be considered as feasible but automatically achieved especially at the register level because of the summation of scalar nonzero and x-vector entry product results to the temporary variable. Spatial locality is feasible, and it is achieved automatically since the y-vector entry results are stored consecutively.

In accessing x-vector entries, both temporal and spatial localities are feasible. Temporal locality is feasible since each x-vector entry may be accessed multiple times. However, exploiting the temporal and spatial localities for the x vector is the major concern in the CSR scheme since x-vector entries are accessed through a *colIndex* array (*colDiff* in ICSR) in a noncontiguous and irregular manner.

2.3. Hypergraph partitioning. A hypergraph $\mathcal{H} = (\mathcal{V}, \mathcal{N})$ is defined as a set $\mathcal{V}$ of vertices and a set $\mathcal{N}$ of nets (hyperedges). Every net $n \in \mathcal{N}$ connects a subset of vertices, i.e., $n \subseteq \mathcal{V}$. Weights and costs can be associated with vertices and nets, respectively. We use $w(v)$ to denote the weight of vertex v and $cost(n)$ to denote the cost of net n. Given a hypergraph $\mathcal{H} = (\mathcal{V}, \mathcal{N})$, $\{\mathcal{V}_1, \ldots, \mathcal{V}_K\}$ is called a K-way partition of the vertex set $\mathcal{V}$ if vertex parts are mutually disjoint and exhaustive. A K-way vertex partition of $\mathcal{H}$ is said to satisfy the balanced-partitioning constraint if $W_k \leq W_{avg}(1 + \varepsilon)$ for $k = 1, \ldots, K$. W_k denotes the weight of a part $\mathcal{V}_k$ and is defined as the sum of weights of vertices in $\mathcal{V}_k$. W_{avg} is the average part weight, and ε represents a predetermined, maximum allowable imbalance ratio.

In a partition of $\mathcal{H}$, a net that connects at least one vertex in a part is said to *connect* that part. *Connectivity* $\lambda(n)$ of a net n denotes the number of parts connected by n. A net n is said to be *cut* if it connects more than one part (i.e., $\lambda(n) > 1$) and *uncut* (*internal*) otherwise (i.e., $\lambda(n) = 1$). The set of cut nets of a partition is denoted as $\mathcal{N}_{cut}$. The partitioning objective is to minimize the cutsize

defined over the cut nets. There are various cutsize definitions. Two relevant cutsize definitions are the cut-net and connectivity metrics [8]:

$$(2.1) \qquad cutsize_{cutnet} = \sum_{n \in \mathcal{N}_{cut}} cost(n), \qquad cutsize_{con} = \sum_{n \in \mathcal{N}_{cut}} \lambda(n) \, cost(n).$$

In the cut-net metric, each cut net n incurs $cost(n)$ to the cutsize, whereas in the connectivity metric, each cut net incurs $\lambda(n) \, cost(n)$ to the cutsize. The HP problem is known to be NP-hard [28]. There exist several successful HP tools such as hMeTiS [26], PaToH [9], and Mondriaan [38], all of which apply the multilevel framework.

The *recursive bisection* (RB) paradigm is widely used in K-way HP and is known to be amenable to producing good solution qualities. In the RB paradigm, first, a 2-way partition of the hypergraph is obtained. Then, each part of the bipartition is further bipartitioned in a recursive manner until the desired number K of parts is obtained or part weights drop below a given part-weight threshold W_{max}. In RB-based HP, the cut-net removal and cut-net splitting schemes [8] are used to capture the cut-net and connectivity cutsize metrics, respectively. The RB paradigm is inherently suitable for partitioning hypergraphs when K is not known in advance. Hence, the RB paradigm can be successfully utilized in clustering rows/columns for cache-size–aware row/column reordering.

2.4. Hypergraph models for sparse matrix partitioning. Recently, several successful hypergraph models have been proposed for partitioning sparse matrices [11, 8]. The relevant ones are row-net, column-net, and row-column-net (fine-grain) models. The row-net and column-net models are used for 1D columnwise and 1D rowwise partitioning of sparse matrices, respectively, whereas the row-column-net model is used for 2D fine-grain partitioning of sparse matrices.

In the row-net hypergraph model [4, 7, 8] $\mathcal{H}_{RN}(A) = (\mathcal{V}_\mathcal{C}, \mathcal{N}_\mathcal{R})$ of matrix A, there exist one vertex $v_j \in \mathcal{V}_\mathcal{C}$ and one net $n_i \in \mathcal{N}_\mathcal{R}$ for each column c_j and row r_i, respectively. The weight $w(v_j)$ of a vertex v_j is set to the number of nonzeros in column c_j. The net n_i connects the vertices corresponding to the columns that have a nonzero entry in row r_i. Every net $n_i \in \mathcal{N}_\mathcal{R}$ has unit cost, i.e., $cost(n_i) = 1$. In the column-net hypergraph model [4, 7, 8] $\mathcal{H}_{CN}(A) = (\mathcal{V}_\mathcal{R}, \mathcal{N}_\mathcal{C})$ of matrix A, there exist one vertex $v_i \in \mathcal{V}_\mathcal{R}$ and one net $n_j \in \mathcal{N}_\mathcal{C}$ for each row r_i and column c_j, respectively. The weight $w(v_i)$ of a vertex v_i is set to the number of nonzeros in row r_i. Net n_j connects the vertices corresponding to the rows that have a nonzero entry in column c_j. Every net n_j has unit cost, i.e., $cost(n_j) = 1$. Note that these two models are duals: the column-net representation of a matrix is equivalent to the row-net representation of its transpose, i.e., $\mathcal{H}_{CN}(A) = \mathcal{H}_{RN}(A^T)$.

In the row-column-net model [11, 10] $\mathcal{H}_{RCN}(A) = (\mathcal{V}_\mathcal{Z}, \mathcal{N}_{\mathcal{RC}})$ of matrix A, there exists one vertex $v_{ij} \in \mathcal{V}_\mathcal{Z}$ corresponding to each nonzero a_{ij} in matrix A. In net set $\mathcal{N}_{\mathcal{RC}}$, there exists a row net n_i^r for each row r_i, and there exists a column net n_j^c for each column c_j. Every row net and column net have unit cost. Row net n_i^r connects the vertices corresponding to the nonzeros in row r_i, and column net n_j^c connects the vertices corresponding to the nonzeros in column c_j. Note that each vertex is connected by exactly two nets, and every pair of nets shares at most one vertex.

A sparse matrix is said to be in columnwise SB form if the rows of diagonal blocks are coupled by columns in the column border, i.e., if each coupling column has nonzeros in the rows of at least two diagonal blocks. A dual definition holds for rowwise SB form. In [4], it is shown that row-net and column-net models can also be

used for transforming a sparse matrix into a K-way SB form through row and column reordering. In particular, the row-net model can be used for permuting a matrix into a rowwise SB form, whereas the column-net model can be used for permuting a matrix into a columnwise SB form. Here we will briefly describe how a K-way partition of the column-net model can be decoded as a row/column reordering for this purpose, and a dual discussion holds for the row-net model.

A K-way vertex partition $\{\mathcal{V}_1, \ldots, \mathcal{V}_K\}$ of $\mathcal{H}_{CN}(A)$ is considered as inducing a $(K + 1)$-way partition $\{\mathcal{N}_1, \ldots, \mathcal{N}_K; \mathcal{N}_{cut}\}$ on the net set of $\mathcal{H}_{CN}(A)$. Here $\mathcal{N}_k$ denotes the set of internal nets of vertex part $\mathcal{V}_k$, whereas $\mathcal{N}_{cut}$ denotes the set of cut nets. The vertex partition is decoded as a partial row reordering of matrix A such that the rows associated with vertices in $\mathcal{V}_{k+1}$ are ordered after the rows associated with vertices $\mathcal{V}_k$ for $k = 1, \ldots, K - 1$. The net partition is decoded as a partial column reordering of matrix A such that the columns associated with nets in $\mathcal{N}_{k+1}$ are ordered after the columns associated with nets in $\mathcal{N}_k$ for $k = 1, \ldots, K-1$, whereas the columns associated with the cut nets are ordered last to constitute the column border.

3. Related work. The main focus of this work is to perform iteration and data reordering, without changing the conventional CSR-based SpMxV codes, whereas cache-aware techniques such as prefetching and blocking are outside the scope of this paper. So we summarize the related work on iteration and data reordering for irregular applications which usually use index arrays to access other arrays. Iteration and data reordering approaches can also be categorized as dynamic and static. Dynamic schemes [12, 13, 15, 19, 34] achieve runtime reordering transformations by analyzing the irregular memory access patterns through adopting an inspector/executor strategy [29]. Reordering rows/columns of irregularly sparse matrices to exploit locality during SpMxV operations can be considered as a static case of such a general iteration/data reordering problem. We call it a static case [32, 36, 40, 41] since the sparsity pattern of matrix A together with the CSR- or CSC-based SpMxV scheme determines the memory access pattern. In the CSR scheme, iteration order corresponds to row order of matrix A and data order corresponds to column order, whereas a dual discussion applies for CSC.

Dynamic and static transformation heuristics differ mainly in the preprocessing times. Fast heuristics are usually used for dynamic reordering transformations, whereas much more sophisticated heuristics are used for the static case. The preprocessing time for the static case can amortize the performance improvement during repeated computations with the same memory access pattern. Repeated SpMxV computations involving the same matrix or matrices with the same sparsity pattern constitute a very typical case of such a static case. In the rest of this section, we focus our discussion on static schemes, whereas a more comprehensive discussion can be found in our technical report [2].

Space-filling curves such as Hilbert and Morton as well as recursive storage schemes such as quadtree are used for iteration reordering in improving locality in dense matrix operations [16, 17, 25] and in sparse matrix operations [18]. Space-filling curves [12] and hierarchical graph clustering [19] are utilized for data reordering in improving locality in n-body simulation applications.

Al-Furaih and Ranka [3] introduce an interaction graph model to investigate optimizations for unstructured iterative applications. They compare several methods to reorder data elements through reordering the vertices of the interaction graph, such as breadth first search (BFS) and graph partitioning. Agarwal, Gustavson, and Zubair [1]

try to improve SpMxV by extracting dense block structures. Their methods consist of examining row blocks to find dense subcolumns and reorder these subcolumns consecutively. Temam and Jalby [35] analyze the cache-miss behavior of SpMxV. They report that the cache-hit ratio decreases as the bandwidth of the sparse matrix increases beyond the cache size, and they conclude that bandwidth reduction algorithms improve cache utilization.

Toledo [36] compares several techniques to reduce cache misses in SpMxV. He uses graph theoretic methods such as Cuthill–McKee (CM), reverse Cuthill–McKee (RCM), and graph partitioning for reordering matrices and other improvement techniques such as blocking, prefetching, and instruction-level-related optimization. He reports that SpMxV performance cannot be improved through row/column reordering. White and Sadayappan [40] discuss data locality issues in SpMxV in detail. They compare SpMxV performance of CSR, CSC, and blocked versions of CSR and CSC. They also propose a graph partitioning based row/column reordering method which is similar to that of Toledo. They report that they could not achieve performance improvement over the original ordering, as also reported by Toledo [36]. Haque and Hossain [20] propose a column reordering method based on the Gray code.

There are several works on row/column reordering based on traveling salesman problem (TSP) formulations. TSP is the well-studied problem of finding the shortest possible route that visits each city exactly once and returns to the origin city. The TSP formulations used for row/column reordering do not require returning to the origin city, and they utilize the objective of path weight maximization instead of path weight minimization. So, in the graph theoretic aspect, this TSP variant is equivalent to finding a maximum-weight path that visits each vertex exactly once in a complete edge-weighted graph. Heras et al. [23] define four distance functions for edge weighting depending on the similarity of sparsity patterns between rows/columns. Pichel et al. [31] use a TSP-based reordering and blocking technique to show improvements in both single processor performance and multicomputer performance. Pichel et al. [30] compare the performance of a number of reordering techniques which utilize TSP, graph partitioning, RCM, and approximate minimum degree.

In a recent work, Yzelman and Bisseling [41] propose a row/column reordering method based on partitioning a row-net hypergraph representation of a given sparse matrix for CSR-based SpMxV. They achieve spatial locality on x-vector entries by clustering the columns with similar sparsity patterns. They also exploit temporal locality for x-vector entries by using the zig-zag property of the ZZCSR and ZZICSR schemes mentioned in section 2.1. This method will be referred to as sHP$_{RN}$ in the rest of the paper.

4. Proposed models and methods. Figure 4.1 displays our taxonomy for reordering methods used to exploit locality in SpMxV operations in order to better identify the proposed as well as the existing methods that are used as baseline methods. As seen in the figure, we investigate single- and multiple-SpMxV frameworks. Reordering methods are categorized as bottom-up and top-down approaches. Methods in the top-down approach are categorized according to the matrix partitioning method utilized. Figure 4.1 shows the hypergraph models used for top-down matrix partitioning methods as well as the graph model used in the bottom-up methods. Figure 4.1 also shows the correspondence between the graph/hypergraph models used in reordering methods for exploiting locality in SpMxV operations and graph/hypergraph models used in data and iteration reordering methods for exploiting locality in other applications in the literature. The leaves of the taxonomy tree show the abbreviations used
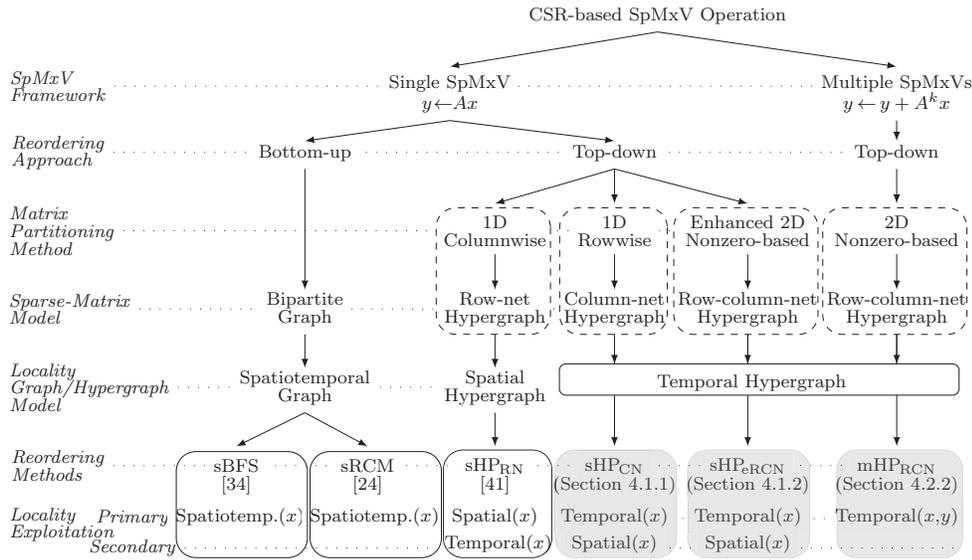
FIG. 4.1. *A taxonomy for reordering methods used to exploit locality in SpMxV operations. Shaded leaves denote proposed methods.*

for existing and proposed methods, together with the temporal/spatial locality exploitation and precedence for the input and/or output vector(s). We should mention that the taxonomy given in Figure 4.1 holds mainly for CSR-based SpMxV, whereas it continues to hold for CSC-based SpMxV by performing 1D rowwise partitioning for sHP$_{RN}$ instead of 1D columnwise partitioning and by performing 1D columnwise partitioning for sHP$_{CN}$ instead of 1D rowwise partitioning. Furthermore, for sHP$_{eRCN}$, enhanced 2D nonzero-based partitioning should be modified accordingly.

In section 4.1, we describe and discuss the proposed two cache-size–aware row/column reordering methods for the single-SpMxV framework. In section 4.2, we describe and discuss the proposed cache-size–aware matrix splitting method for the multiple-SpMxV framework.

4.1. Single-SpMxV framework. In this framework, the y-vector results are computed by performing a single SpMxV operation, i.e., $y \leftarrow Ax$. The objective in this scheme is to reorder the columns and rows of matrix A for maximizing the exploitation of temporal and spatial localities in accessing x-vector entries. That is, the objective is to find row and column permutation matrices P_r and P_c so that $y \leftarrow Ax$ is computed as $\hat{y} \leftarrow \hat{A}\hat{x}$, where $\hat{A} = P_r A P_c$, $\hat{x} = x P_c$, and $\hat{y} = P_r\, y$. For the sake of simplicity of presentation, reordered input and output vectors $\hat{x}$ and $\hat{y}$ will be referred to as x and y in the rest of the paper.

Recall that temporal locality in accessing y-vector entries is not feasible, whereas spatial locality is achieved automatically because y-vector results are stored and processed consecutively. Reordering the rows with similar sparsity patterns nearby increases the possibility of exploiting temporal locality in accessing x-vector entries. Reordering the columns with similar sparsity patterns nearby increases the possibility of exploiting spatial locality in accessing x-vector entries. This row/column reordering problem can also be considered as a row/column clustering problem, and this clustering process can be achieved in two distinct ways: top-down and bottom-up.

In this section, we propose and discuss cache-size–aware top-down approaches based on 1D and 2D partitioning of a given matrix. Although a bottom-up approach based on hierarchical clustering of rows/columns with similar patterns is feasible, such a scheme is not discussed in this work.

In sections 4.1.1 and 4.1.2, we present two theorems that give the guidelines for a "good" cache-size–aware row/column reordering based on 1D and 2D matrix partitioning. These theorems provide upper bounds on the number of cache misses due to the access of x-vector entries in the SpMxV operation performed on sparse matrices in two special forms, namely, SB and DB forms. In these theorems, $\Phi_x(A)$ denotes the number of cache misses due to the access of x-vector entries in a CSR-based SpMxV operation to be performed on matrix A.

In the theorems given in sections 4.1 and 4.2, fully associative cache is assumed, since misses in a fully associative cache are capacity misses and are not conflict misses. That is, each data line in the main memory can be placed to any empty line in the fully associative cache without causing a conflict miss. In these theorems, a matrix/submatrix is said to fit into the cache if the size of the CSR storage of the matrix/submatrix together with the associated x and y vectors/subvectors is smaller than the size of the cache.

4.1.1. Row/column reordering based on 1D matrix partitioning. We consider a row/column reordering which permutes a given matrix A into a K-way columnwise SB form

$$\hat{A} = A_{SB} = P_r A P_c = \begin{bmatrix} A_{11} & & & & A_{1B} \\ & A_{22} & & & A_{2B} \\ & & \ddots & & \vdots \\ & & & A_{KK} & A_{KB} \end{bmatrix} = \begin{bmatrix} R_1 \\ R_2 \\ \vdots \\ R_K \end{bmatrix}$$

$$(4.1) \qquad\qquad = \begin{bmatrix} C_1 & C_2 & \ldots & C_K & C_B \end{bmatrix}.$$

Here, A_{kk} denotes the kth diagonal block of A_{SB}. $R_k = [0 \ldots 0 \ A_{kk} \ 0 \ldots 0 \ A_{kB}]$ denotes the kth row slice of A_{SB} for $k = 1, \ldots, K$. $C_k = \begin{bmatrix} 0 \ldots 0 \ A_{kk}^T \ 0 \ldots 0 \end{bmatrix}^T$ denotes the kth column slice of A_{SB} for $k = 1, \ldots, K$, and C_B denotes the column border as follows:

$$(4.2) \qquad\qquad C_B = \begin{bmatrix} A_{1B} \\ A_{2B} \\ \vdots \\ A_{KB} \end{bmatrix}.$$

Each column in the border C_B is called a *row-coupling column* or simply a *coupling column*. Let $\lambda(c_j)$ denote the number of R_k submatrices that contain at least one nonzero of column c_j of matrix A_{SB}, i.e.,

$$(4.3) \qquad\qquad \lambda(c_j) = |\{R_k \in A_{SB} : c_j \in R_k\}|.$$

In other words, $\lambda(c_j)$ denotes the row-slice connectivity or simply connectivity of column c_j in A_{SB}. Note that $\lambda(c_j)$ varies between 1 and K. In this notation, a column c_j is a coupling column if $\lambda(c_j) > 1$. Here and hereafter, a submatrix notation is interchangeably used to denote both a submatrix and the set of nonempty rows/columns that belong to that matrix. For example, in (4.3), R_k denotes both the kth row slice of A_{SB} and the set of columns that belong to submatrix R_k.

The individual $y \leftarrow Ax$ can be equivalently represented as K output-independent but input-dependent SpMxV operations, i.e., $y_k \leftarrow R_k x$ for $k = 1, \ldots, K$, where each submatrix R_k is assumed to be stored in the CSR scheme. These SpMxV operations are input-dependent because of the x-vector entries corresponding to the coupling columns.

THEOREM 4.1. *Given a K-way SB form A_{SB} of matrix A such that each submatrix R_k fits into the cache, we have*

$$(4.4) \qquad\qquad \Phi_x(A_{SB}) \leq \sum_{c_j \in A_{SB}} \lambda(c_j).$$

Proof. Since each submatrix R_k fits into the cache, for each $c_j \in R_k$, x_j will be loaded to the cache at most once during the $y_k \leftarrow R_k x$ multiply. Therefore, for a column c_j, the maximum number of cache misses that can occur due to the access of x_j is bounded above by $\lambda(c_j)$. Note that this worst case happens when no cache reuse occurs in accessing x-vector entries during successive $y_k \leftarrow R_k x$ operations implicitly performed in $y \leftarrow Ax$. $\square$

Theorem 4.1 leads us to a cache-size–aware top-down row/column reordering through an A-to-A_{SB} transformation that minimizes the upper bound given in (4.4) for $\Phi_x(A_{SB})$. Minimizing this sum relates to minimizing the number of cache misses due to the loss of temporal locality.

This A-to-A_{SB} transformation problem can be formulated as an HP problem using the column-net model of matrix A with the part size constraint of cache size and the partitioning objective of minimizing cutsize according to the connectivity metric definition given in (2.1). In this way, minimizing the cutsize corresponds to minimizing the upper bound given in Theorem 4.1 for the number of cache misses due to the access of x-vector entries. This proposed reordering method will be referred to as "sHP$_{CN}$," where the lowercase letter "s" is used to indicate the single-SpMxV framework.

Exploiting temporal versus spatial locality in SpMxV. Here we compare and contrast the existing HP-based method [41] sHP$_{RN}$ and the proposed method sHP$_{CN}$ in terms exploiting temporal and spatial localities. Both sHP$_{RN}$ and sHP$_{CN}$ belong to the single-SpMxV framework and utilize 1D matrix partitioning for row/column reordering. For the CSR-based SpMxV operation, the row-net model utilized by sHP$_{RN}$ corresponds to the spatial locality hypergraph model proposed by Strout and Hovland [34] for data reordering of unstructured mesh computations. On the other hand, the column-net model utilized by sHP$_{CN}$ corresponds to the temporal locality hypergraph proposed by Strout and Hovland [34] for iteration reordering. Here, iteration reordering refers to changing the order of computation that accesses specific data, and data reordering refers to changing the assignment of data to memory locations so that accesses to the same or nearby locations occur relatively closely in time throughout the computations. Note that in the CSR-based SpMxV, the inner products of sparse rows with the dense input vector x correspond to the iterations to be reordered. So the major difference between the sHP$_{RN}$ and sHP$_{CN}$ methods is that sHP$_{RN}$ considers exploiting primarily spatial locality and secondarily temporal locality, whereas sHP$_{CN}$ considers the reverse.

The above-mentioned difference between sHP$_{RN}$ and sHP$_{CN}$ can also be observed by investigating the row-net and column-net models used in these two HP-based methods. In HP with connectivity metric, the objective of cutsize minimization corresponds to clustering vertices with similar net connectivity to the same vertex parts.

Hence, sHP_{RN} clusters columns with similar sparsity patterns to the same column slice for partial column reordering, thus exploiting spatial locality primarily, whereas sHP_{CN} clusters rows with similar sparsity patterns to the same row slice for partial row reordering, thus exploiting temporal locality primarily. In sHP_{RN}, the uncut and cut nets of a partition are used to decode the partial row reordering, thus exploiting temporal locality secondarily. In sHP_{CN}, the uncut and cut nets of a partition are used to decode the partial column reordering, thus exploiting spatial locality secondarily.

We should also note that the row-net and column-net models become equivalent for symmetric matrices. So, sHP_{RN} and sHP_{CN} obtain the same vertex partitions for symmetric matrices. The difference between these two methods in reordering matrices stems from the difference in the way that they decode the resultant partitions. sHP_{RN} reorders the columns corresponding to the vertices in the same part of a partition successively, whereas sHP_{CN} reorders the rows corresponding to the vertices in the same part of a partition successively.

4.1.2. Row/column reordering based on 2D matrix partitioning. We consider a row/column reordering which permutes a given matrix A into a K-way DB form

$$\hat{A} = A_{DB} = P_r A P_c = \begin{bmatrix} A_{11} & & & & A_{1B} \\ & A_{22} & & & A_{2B} \\ & & \ddots & & \vdots \\ & & & A_{KK} & A_{KB} \\ A_{B1} & A_{B2} & \dots & A_{BK} & A_{BB} \end{bmatrix} = \begin{bmatrix} R_1 \\ R_2 \\ \vdots \\ R_K \\ R_B \end{bmatrix} = \begin{bmatrix} A'_{SB} \\ R_B \end{bmatrix}$$

$$(4.5) \qquad = \begin{bmatrix} C_1 & C_2 & \dots & C_K & C_B \end{bmatrix}.$$

Here, $R_B = [A_{B1}\ A_{B2}\ \dots\ A_{BK}\ A_{BB}]$ denotes the row border. Each row in R_B is called a *column-coupling row* or simply a *coupling row*. A'_{SB} denotes the columnwise SB part of A_{DB} excluding the row border R_B. R_k denotes the kth row slice of both A'_{SB} and A_{DB}. $\lambda'(c_j)$ denotes the connectivity of column c_j in A'_{SB}. C'_B denotes the column border of A'_{SB}, whereas $C_B = [C'^T_B\ A^T_{BB}]^T$ denotes the column border of A_{DB}. $C_k = \begin{bmatrix} 0 \dots 0\ A^T_{kk}\ 0 \dots 0\ A^T_{Bk} \end{bmatrix}^T$ denotes the kth column slice of A_{DB}. Let $nnz(r_i)$ denote the number of nonzeros in row r_i.

THEOREM 4.2. *Given a K-way DB form A_{DB} of matrix A such that each submatrix R_k of A'_{SB} fits into the cache, we have*

$$(4.6) \qquad \Phi_x(A_{DB}) \leq \sum_{c_j \in A'_{SB}} \lambda'(c_j) + \sum_{r_i \in R_B} nnz(r_i).$$

Proof. We can consider the $y \leftarrow Ax$ multiply as two output-independent but input-dependent SpMxVs: $y_{SB} \leftarrow A'_{SB} x$ and $y_B \leftarrow R_B x$, where $y = [y^T_{SB}\ y^T_B]^T$. Thus $\Phi_x(A_{DB}) \leq \Phi_x(A'_{SB}) + \Phi_x(R_B)$. This upper bound occurs when no cache reuse happens in accessing x-vector entries between the former and latter SpMxV operations. By the proof of Theorem 4.1, we already have $\Phi_x(A'_{SB}) \leq \sum_{c_j} \lambda'(c_j)$. In the $y_B \leftarrow R_B x$ multiply, we have at most $nnz(r_i)$ x-vector accesses for each column-coupling row r_i of R_B. This worst case happens when no cache reuse occurs in accessing x-vector entries during the $y_B \leftarrow R_B x$ multiply. Hence, $\Phi_x(R_B) \leq \sum_{r_i \in R_B} nnz(r_i)$, thus concluding the proof. $\square$

Theorem 4.2 leads us to a cache-size–aware top-down row/column reordering through an A-to-A_{DB} transformation that minimizes the upper bound given in (4.6)

for $\Phi_x(A_{DB})$. Here, minimizing this sum relates to minimizing the number of cache misses due to the loss of temporal locality.

Here we propose to formulate the above-mentioned A-to-A_{DB} transformation problem as an HP problem using the row-column-net model of matrix A with a part size constraint of cache size. In the proposed formulation, column nets are associated with unit cost (i.e., $cost(n_j^c) = 1$ for each column c_j), and the cost of each row net is set to the number of nonzeros in the respective row (i.e., $cost(n_i^r) = nnz(r_i)$). However, existing HP tools do not handle a cutsize definition that encapsulates the right-hand side of (4.6), because the connectivity metric should be enforced for column nets, whereas the cut-net metric should be enforced for row nets. In order to encapsulate this different cutsize definition, we adapt and enhance the cut-net removal and cut-net splitting techniques adopted in RB algorithms utilized in HP tools. The connectivity of a column net should be calculated in such a way that it is as close as possible to the connectivity of the respective coupling column in the A'_{SB} part of A_{DB}. For this purpose, after each bipartitioning step, each cut row net is removed together with all vertices that it connects in both sides of the bipartition. Recall that the vertices of a cut net are not removed in the conventional cut-net removal scheme [8]. After applying the proposed removal scheme on the row nets on the cut, the conventional cut-net splitting technique [8] is applied to the column nets on the cut of the bipartition. This enhanced row-column-net model will be abbreviated as the "eRCN" model and the resulting reordering method will be referred to as "sHP$_{\text{eRCN}}$."

The K-way partition $\{\mathcal{V}_1, \ldots, \mathcal{V}_K\}$ of $\mathcal{H}_{RCN}(A)$ obtained as a result of the above-mentioned RB process is decoded as follows to induce a desired DB form of matrix A. The rows corresponding to the cut row nets are permuted to the end to constitute the coupling rows of the row border R_B. The rows corresponding to the internal row nets of part $\mathcal{V}_k$ are permuted to the kth row slice R_k. The columns corresponding to the internal column nets of part $\mathcal{V}_k$ are permuted to the kth column slice C_k. It is clear that the columns corresponding to the cut column nets remain in the column border C_B of A_{DB}, and hence only those columns have the potential to remain in the column border C'_B of A'_{SB}. Some of these columns may be permuted to a column slice C_k if all of its nonzeros become confined to row slice R_k and row border R_B. Such cases may occur as follows: Consider a cut column net n_j^c of a bipartition obtained at a particular RB step. If the internal row nets that belong to one part of the bipartition and that share a vertex with n_j^c all become cut nets in the following RB steps, then column c_j may no longer be a coupling column and may be safely permuted to column slice C_k. For such cases, the proposed scheme fails to correctly encapsulate the column connectivity cost in A'_{SB}. The proposed cut row-net removal scheme avoids such column-connectivity miscalculations that may occur in future RB steps due to the cut row nets of the current bipartition. However, it is clear that our scheme cannot avoid such possible errors (related to the cut column nets of the current bipartition) that may occur due to the row nets to be cut in future RB steps.

Similar to sHP$_{\text{CN}}$, the sHP$_{\text{eRCN}}$ method clusters rows with similar sparsity patterns to the same row slice for partial row reordering, thus exploiting temporal locality primarily, and also the uncut and cut column nets of a partition are used to decode the partial column reordering, thus exploiting spatial locality secondarily.

4.2. Multiple-SpMxV framework. Let $\Pi = \{A^1, A^2, \ldots, A^K\}$ denote a splitting of matrix A into K A^k matrices, where $A = A^1 + A^2 + \cdots + A^K$. In Π, A^k matrices are mutually nonzero disjoint; however, they are not necessarily row

disjoint or column disjoint. In this framework, the $y \leftarrow Ax$ operation is computed as a sequence of K input- and output-dependent SpMxV operations, $y \leftarrow y + A^k x$ for $k = 1, \ldots, K$. Individual SpMxV results are accumulated in the output vector y on the fly in order to avoid additional write operations. The individual SpMxV operations are input-dependent because of the shared columns among the A^k matrices, whereas they are output-dependent because of the shared rows among the A^k matrices. Note that A^k matrices are likely to contain empty rows and columns. The splitting of matrix A should be done in such a way that the temporal and spatial localities of individual SpMxVs are exploited in order to minimize the number of cache misses.

We discuss pros and cons of this framework compared to the single-SpMxV framework in section 4.2.1. In section 4.2.2, we present a theorem that gives the guidelines for a "good" cache-size–aware matrix splitting based on 2D matrix partitioning. This theorem provides an upper bound on the total number of cache misses due to the access of x-vector and y-vector entries in all $y \leftarrow y + A^k x$ operations. The order of individual SpMxV operations is also important to exploit temporal locality between consecutive $y \leftarrow y + A^k x$ operations. In section 4.2.3, we propose and discuss two methods for ordering SpMxV operations: RB ordering and TSP ordering.

4.2.1. Pros and cons compared to single-SpMxV framework. In the multiple-SpMxV framework, every splitting defines an access order on the matrix nonzeros, and every access order on the matrix nonzeros can define a splitting that causes it. Note that not all nonzero access orders can be achieved by row reordering. So the single-SpMxV framework can be considered as a special case of the multiple-SpMxV framework in which A^k matrices are restricted to being row disjoint. Thus, the multiple-SpMxV framework brings an additional flexibility for exploiting temporal locality. Clustering A-matrix rows/subrows with similar sparsity patterns into the same A^k matrices increases the possibility of exploiting temporal locality in accessing x-vector entries. Clustering A-matrix columns/subcolumns with similar sparsity patterns into the same A^k matrices increases the possibility of exploiting temporal locality in accessing y-vector entries.

It is clear that the single-SpMxV framework utilizing the CSR scheme suffers severely from dense rows. Dense rows cause loading a large number of x-vector entries to the cache, thus disturbing the temporal locality in accessing x-vector entries. The multiple-SpMxV framework may overcome this deficiency of the single-SpMxV framework through utilizing the flexibility of distributing the nonzeros of dense rows among multiple A^k matrices in such a way as to exploit the temporal locality in the respective $y \leftarrow y + A^k x$ operations.

However, this additional flexibility comes at the cost of disturbing the following localities compared to the single SpMxV approach. There is some disturbance in the spatial locality in accessing the nonzeros of the A matrix due to the division of three arrays associated with nonzeros into K parts. However, this disturbance in spatial locality is negligible since elements of each of the three arrays are stored and accessed consecutively during each SpMxV operation. That is, at most $3(K-1)$ extra cache misses occur compared to the single SpMxV scheme due to the disturbance of spatial locality in accessing the nonzeros of the A matrix. More importantly, multiple read/writes of the individual SpMxV results might bring some disadvantages compared to the single SpMxV scheme. These multiple read/writes disturb the spatial locality of accessing y-vector entries as well as introducing a temporal locality exploitation problem in y-vector entries.

4.2.2. Splitting A into A^k matrices based on 2D matrix partitioning.
Given a splitting Π of matrix A, let $\Phi_x(A, \Pi)$ and $\Phi_y(A, \Pi)$, respectively, denote the number of cache misses due to the access of x-vector and y-vector entries during $y \leftarrow y + A^k x$ operations for $k = 1, \ldots, K$. Here, the total number of cache misses can be expressed as $\Phi(A, \Pi) = \Phi_x(A, \Pi) + \Phi_y(A, \Pi)$. Let $\lambda(r_i)$ and $\lambda(c_j)$, respectively, denote the number of A^k matrices that contain at least one nonzero of row r_i and one nonzero of column c_j of matrix A, i.e.,

$$(4.7a) \qquad\qquad \lambda(r_i) = |\{A^k \in \Pi : r_i \in A^k\}|,$$

$$(4.7b) \qquad\qquad \lambda(c_j) = |\{A^k \in \Pi : c_j \in A^k\}|.$$

THEOREM 4.3. *Given a splitting* $\Pi = \{A^1, A^2, \ldots, A^K\}$ *of matrix* A *such that each* A^k *matrix fits into the cache, we have*
   (a) $\Phi_x(A, \Pi) \leq \sum_{c_j \in A} \lambda(c_j)$;
   (b) $\Phi_y(A, \Pi) \leq \sum_{r_i \in A} \lambda(r_i)$.

Proof of (a). Since each matrix A^k fits into the cache, for any $c_j \in A^k$, the number of cache misses due to the access of x_j is at most $\lambda(c_j)$ during all $y \leftarrow y + A^k x$ operations. This worst case happens when no cache reuse occurs in accessing x_j during successive $y \leftarrow y + A^k x$ operations.

Proof of (b). For any $r_i \in A^k$, the number of cache misses due to the access of y_i is at most $\lambda(r_i)$ during all $y \leftarrow y + A^k x$ operations due to the nature of CSR-based SpMxV computation. This worst case happens when no cache reuse occurs in accessing y_i during successive $y \leftarrow y + A^k x$ operations. $\square$

COROLLARY 4.4. *If each* A^k *in* Π *fits into the cache, then we have*

$$(4.8) \qquad\qquad \Phi(A, \Pi) \leq \sum_{r_i \in A} \lambda(r_i) + \sum_{c_j \in A} \lambda(c_j).$$

Corollary 4.4 leads us to a cache-size–aware top-down matrix splitting that minimizes the upper bound given in (4.8) for $\Phi(A, \Pi)$. Here, minimizing this sum relates to minimizing the number of cache misses due to the loss of temporal locality.

The matrix splitting problem can be formulated as an HP-based 2D matrix partitioning using the row-column-net model of matrix A with a part size constraint of cache size and partitioning objective of minimizing cutsize according to the connectivity metric definition given in (2.1). In this way, minimizing the cutsize corresponds to minimizing the upper bound given in Corollary 4.4 for the total number of cache misses due to the access of x-vector and y-vector entries. This reordering method will be referred to as "mHP$_{\mathrm{RCN}}$," where the lowercase letter "m" is used to indicate the multiple-SpMxV framework.

4.2.3. Ordering individual SpMxV operations. The above-mentioned objective in splitting matrix A into A^k matrices is to exploit the temporal locality of individual SpMxVs in order to minimize the number of cache misses. However, when all SpMxVs are considered, data reuse between two consecutive SpMxVs should be considered to better exploit temporal locality. Here we propose and discuss two methods for ordering SpMxV operations: RB ordering and TSP ordering.

RB ordering. The RB tree constructed during the recursive hypergraph bipartitioning is a full binary tree, where each node represents a vertex subset as well as the respective induced subhypergraph on which a 2-way HP is to be applied. Note that the root node represents both the original vertex set and the original row-column-net

hypergraph model for the given A matrix and the leaf nodes represent the A^k matrices. The preorder, postorder, and in-order traversals starting from the root node give the same traversal order on the leaf nodes, thus inducing an RB order on the individual SpMxV operations of the multiple-SpMxV framework. In the RB tree, the amount of row/column sharing between two leaf nodes (A^k matrices) is expected to decrease with increasing path length to their first common ancestor in the RB tree. Since sibling nodes have a common parent, the A^k matrices corresponding to the sibling leaf-node pairs are likely to share a larger number of rows and columns compared to A^k matrices corresponding to the nonsibling leaf node pairs. As this scheme orders the sibling leaf nodes consecutively, the RB ordering is expected to yield an order on the A^k matrices that respects temporal locality in accessing x-vector and y-vector entries.

TSP ordering. Let $\widehat{\Pi} = \langle A^1, A^2, \ldots, A^K \rangle$ denote an ordered version of a given splitting Π. A subchain of $\widehat{\Pi}$ is said to cover a row r_i and a column c_j if each A^k matrix in the subchain contains at least one nonzero of row r_i and column c_j, respectively. Let $\gamma(r_i)$ and $\gamma(c_j)$ denote the number of maximal A^k matrix subchains that cover row r_i and column c_j, respectively. Let L denote the cache line size. Let $\Phi(A, \widehat{\Pi})$ denote the total number of cache misses due to the access of x-vector and y-vector entries for a given order $\widehat{\Pi}$ of $y \leftarrow y + A^k x$ operations for $k = 1, \ldots, K$. Theorem 4.5 gives a lower bound for $\Phi(A, \widehat{\Pi})$, and Theorem 4.6 shows our TSP formulation that minimizes this lower bound.

THEOREM 4.5. *Given an ordered splitting $\widehat{\Pi}$ of matrix A such that none of the A^k matrices fit into the cache, we have*

$$(4.9) \qquad \Phi(A, \widehat{\Pi}) \geq \frac{\sum_{r_i \in A} \gamma(r_i) + \sum_{c_j \in A} \gamma(c_j)}{L}.$$

Proof. We first consider the case $L = 1$. Consider a column c_j of matrix A. Then there exist $\gamma(c_j)$ maximal A^k matrix subchains that cover column c_j. Since none of the A^k matrices can fit into the cache, it is guaranteed that there will be no cache reuse of column c_j between two different maximal A^k matrix subchains that cover c_j. Therefore, at least $\gamma(c_j)$ cache misses will occur for each column c_j, which means that $\Phi_x(A, \widehat{\Pi}) \geq \sum_{c_j} \gamma(c_j)$. A similar proof follows for a row r_i of matrix A so that $\Phi_y(A, \widehat{\Pi}) \geq \sum_{r_i} \gamma(r_i)$. When $L > 1$, the number of cache misses may decrease L-fold at most. □

As in all top-down approaches, in the mHP$_{\text{RCN}}$ method, matrices are partitioned until the size of the CSR storage of the matrix together with the associated x and y vectors is slightly smaller than the size of the cache. This automatically achieves the upper bounds given in Theorem 4.3 and Corollary 4.4. As the matrices are slightly smaller than the cache size, we hypothesize that the lower bound given in Theorem 4.5 will still relate to the realized cache-miss count.

We define the TSP instance $(\mathcal{G} = (\mathcal{V}, \mathcal{E}), w)$ over a given unordered splitting Π of matrix A as follows. The vertex set $\mathcal{V}$ denotes the set of A^k matrices. The weight $w(k, \ell)$ of edge $e_{k\ell} \in \mathcal{E}$ is set to be equal to the sum of the number of shared rows and columns between A^k and A^ℓ.

THEOREM 4.6. *For a given unordered splitting Π of matrix A, finding an order on the vertices of the TSP instance $(\mathcal{G}, w)$ that maximizes the path weight corresponds to finding an order $\widehat{\Pi}$ of A^k matrices that minimizes the lower bound given in (4.9) for $\Phi(A, \widehat{\Pi})$.*

The proof of Theorem 4.6 can be found in our technical report [2].

5. Experimental results.

5.1. Experimental setup. We tested the performance of the proposed methods against three state-of-the-art methods, sBFS [34], sRCM [13, 24, 36], and sHP_{RN} [41], all of which belong to the single-SpMxV framework. Here, sBFS refers to our adaptation of the BFS-based simultaneous data and iteration reordering method of Strout and Hovland [34] to matrix row and column reordering. Strout and Hovland's method depends on implementing BFS on both temporal and spatial locality hypergraphs simultaneously. In our adaptation, we apply BFS on the bipartite graph representation of the matrix, so that the resulting BFS orders on the row and column vertices determine row and column reorderings, respectively. sRCM refers to applying the RCM method, which is widely used for envelope reduction of symmetric matrices, on the bipartite graph representation of the given sparse matrix. Application of the RCM method to bipartite graphs has also been used by Berry, Hendrickson, and Raghavan [6] to reorder rectangular term-by-document matrices for envelope minimization. sHP_{RN} refers to the work by Yzelman and Bisseling [41], which utilizes HP using the row-net model for CSR-based SpMxV.

The HP-based top-down reordering methods sHP_{RN}, sHP_{CN}, sHP_{eRCN}, and mHP_{RCN} are implemented using the state-of-the-art HP tool PaToH [9]. In these implementations, PaToH is used as a 2-way HP tool within the RB paradigm. The hypergraphs representing sparse matrices according to the respective models are recursively bipartitioned into parts until the CSR storage size of the matrix/submatrix (together with the associated x and y vectors/subvectors) corresponding to a part drops below the cache size. PaToH is used with default parameters except the use of heavy connectivity clustering (`PATOH_CRS_HCC=9`) in the sHP_{RN}, sHP_{CN}, and sHP_{eRCN} methods that belong to the single-SpMxV framework, and the use of absorption clustering using nets (`PATOH_CRS_ABSHCC=11`) in the mHP_{RCN} method that belong to the multiple-SpMxV framework. Since PaToH contains randomized algorithms, the reordering results are reported by averaging the values obtained in 10 different runs, each randomly seeded.

Performance evaluations are carried out in two different settings: cache-miss simulations and actual runtimes by using OSKI [39]. In cache-miss simulations, eight-byte words are used for matrix nonzeros, x-vector entries, and y-vector entries. In OSKI runs, double precision arithmetic is used. Cache-miss simulations are performed on 36 small-to-medium size matrices, whereas OSKI runs are performed on 17 large size matrices. All test matrices are obtained from the University of Florida Sparse Matrix Collection [14]. CSR storage sizes of small-to-medium size matrices vary between 441 KB to 13 MB, whereas CSR storage sizes of large size matrices vary between 13 MB to 94 MB. Properties of these matrices are presented in Table 5.1. As seen in the table, both sets of small-to-medium and large size matrices are categorized into three groups as symmetric, square nonsymmetric, and rectangular. In each group, the test matrices are listed in the order of increasing number of nonzeros ("nnz"). In the table, "avg" and "max" denote the average and the maximum number of nonzeros per row/column. "cov" denotes the coefficient of variation of the number of nonzeros per row/column. The "cov" value of a matrix can be considered as an indication of the level of irregularity in the number of nonzeros per row and column.

5.2. Cache-miss simulations. Cache-miss simulations are performed by running the single-level cache simulator developed by Yzelman and Bisseling [41] on small-to-medium size test matrices. The simulator is configured to have a 64 KB, 2-way set-associative cache with a line size of 64 bytes (eight words). Some of the

TABLE 5.1
Properties of test matrices.

Name	Number of			nnz's in a row			nnz's in a column		
	rows	cols	nonzeros	avg	max	cov	avg	max	cov
Small-to-medium size matrices									
Symmetric matrices									
ncvxqp9	16,554	16,554	54,040	3	9	0.5	3	9	0.5
tuma1	22,967	22,967	87,760	4	5	0.3	4	5	0.3
bloweybl	30,003	30,003	120,000	4	10,001	14.4	4	10,001	14.4
bloweya	30,004	30,004	150,009	5	10,001	11.6	5	10,001	11.6
brainpc2	27,607	27,607	179,395	7	13,799	20.2	7	13,799	20.2
a5esindl	60,008	60,008	255,004	4	9,993	12.7	4	9,993	12.7
dixmaanl	60,000	60,000	299,998	5	5	0.0	5	5	0.0
shallow_water1	81,920	81,920	327,680	4	4	0.0	4	4	0.0
c-65	48,066	48,066	360,528	8	3,276	2.5	8	3,276	2.5
finan512	74,752	74,752	596,992	8	55	0.8	8	55	0.8
copter2	55,476	55,476	759,952	14	45	0.3	14	45	0.3
msc23052	23,052	23,052	1,154,814	50	178	0.2	50	178	0.2
Square nonsymmetric matrices									
poli_large	15,575	15,575	33,074	2	491	4.2	2	18	0.2
powersim	15,838	15,838	67,562	4	40	0.6	4	41	0.8
memplus	17,758	17,758	126,150	7	574	3.1	7	574	3.1
Zhao1	33,861	33,861	166,453	5	6	0.1	5	7	0.2
mult_dcop_01	25,187	25,187	193,276	8	22,767	18.7	8	22,774	18.8
jan99jac120sc	41,374	41,374	260,202	6	68	1.1	6	138	2.3
circuit_4	80,209	80,209	307,604	4	6,750	7.8	4	8,900	10.5
ckt11752_dc_1	49,702	49,702	333,029	7	2,921	3.5	7	2,921	3.5
poisson3Da	13,514	13,514	352,762	26	110	0.5	26	110	0.5
bcircuit	68,902	68,902	375,558	6	34	0.4	6	34	0.4
g7jac120	35,550	35,550	475,296	13	153	1.7	13	120	1.7
e40r0100	17,281	17,281	553,562	32	62	0.5	32	62	0.5
Rectangular matrices									
lp_dfl001	6,071	12,230	35,632	6	228	1.3	3	14	0.4
ge	10,099	16,369	44,825	4	48	0.8	3	36	0.9
ex3sta1	17,443	17,516	68,779	4	8	0.4	4	46	1.4
lp_stocfor3	16,675	23,541	76,473	5	15	0.7	3	18	1.0
cq9	9,278	21,534	96,653	10	391	3.5	5	24	1.0
psse0	26,722	11,028	102,432	4	4	0.1	9	68	0.7
co9	10,789	22,924	109,651	10	441	3.6	5	28	1.1
baxter	27,441	30,733	111,576	4	2,951	8.7	4	46	1.6
graphics	29,493	11,822	117,954	4	4	0.0	10	87	1.0
fome12	24,284	48,920	142,528	6	228	1.3	3	14	0.4
route	20,894	43,019	206,782	10	2,781	7.1	5	44	1.0
fxm4_6	22,400	47,185	265,442	12	57	1.0	6	24	1.1
Large size matrices									
Symmetric matrices									
c-73	169,422	169,422	1,279,274	8	39,937	20.1	8	39,937	20.1
c-73b	169,422	169,422	1,279,274	8	39,937	20.1	8	39,937	20.1
rgg_n_2_17_s0	131,072	131,072	1,457,506	11	96	0.3	11	28	0.3
boyd2	466,316	466,316	1,500,397	3	93,262	60.6	3	93,262	60.6
ins2	309,412	309,412	2,751,484	9	303,879	65.3	9	309,412	66.4
rgg_n_2_18_s0	262,144	262,144	3,094,566	12	62	0.3	12	31	0.3
Square nonsymmetric matrices									
Raj1	263,743	263,743	1,302,464	5	40,468	17.9	5	40,468	17.9
rajat21	411,676	411,676	1,893,370	5	118,689	41.0	5	100,470	34.8
rajat24	358,172	358,172	1,948,235	5	105,296	33.1	5	105,296	33.1
ASIC_320k	321,821	321,821	2,635,364	8	203,800	61.4	8	203,800	61.4
Stanford_Berkeley	683,446	683,446	7,583,376	11	76,162	25.0	11	249	1.5
Rectangular matrices									
kneser_10_4_1	349,651	330,751	992,252	3	51,751	31.9	3	3	0.0
neos	479,119	515,905	1,526,794	3	29	0.2	3	16,220	15.6
wheel_601	902,103	723,605	2,170,814	2	442,477	193.9	3	3	0.0
LargeRegFile	2,111,154	801,374	4,944,201	2	4	0.3	6	655,876	145.9
cont1_l	1,918,399	1,921,596	7,031,999	4	5	0.3	4	1,279,998	252.3
degme	185,501	659,415	8,127,528	44	624,079	33.1	12	18	0.1

TABLE 5.2

Average simulation results (misses) to display the merits of enhancement of the row-column-net model in sHP$_{eRCN}$ (cache size = part-weight threshold = 64 KB).

	sHP$_{RCN}$	sHP$_{eRCN}$
	x	x
Symmetric	0.54	0.47
Nonsymmetric	0.45	0.40
Rectangular	0.44	0.43
Overall	0.48	0.43

TABLE 5.3

Average simulation results (misses) to display the merits of ordering SpMxV operations in mHP$_{RCN}$ (cache size = part-weight threshold = 64 KB).

	Random ordering			RB ordering			TSP ordering		
	x	y	$x+y$	x	y	$x+y$	x	y	$x+y$
Symmetric	0.44	1.34	0.62	0.41	1.28	0.58	0.40	1.26	0.57
Nonsymmetric	0.37	1.60	0.54	0.34	1.55	0.50	0.34	1.54	0.50
Rectangular	0.27	1.39	0.40	0.26	1.35	0.39	0.27	1.36	0.40
Overall	0.35	1.44	0.51	0.33	1.39	0.49	0.33	1.38	0.48

experiments are conducted to show the sensitivities of the methods to the cache-line size without changing the other cache parameters. In the simulations, since the ICSR [27] storage scheme is to be used in the multiple-SpMxV framework as discussed in section 4.2, ICSR is also used for all other methods. The ZZCSR scheme proposed by Yzelman and Bisseling [41] is not used in the simulations, since the main purpose of this work is to show the cache-miss effects of the six different reordering methods. In Tables 5.2, 5.3, 5.4, and 5.7, the performances of the existing and proposed methods are displayed in terms of normalized cache-miss values, where each normalized value is calculated through dividing the number of cache misses for the reordered matrix by that of the original matrix. In these tables, the x, y, and $x + y$ columns, respectively, denote the normalized cache-miss values due to the access of x-vector entries, y-vector entries, and both. In these tables, compulsory cache misses due to the access of matrix nonzeros are not reported in order to better show the performance differences among the methods.

We introduce Table 5.2 to show the validity of the enhanced row-column-net model proposed in section 4.1.2 for the sHP$_{eRCN}$ method. In the table, sHP$_{RCN}$ refers to a version of the sHP$_{eRCN}$ method that utilizes the conventional row-column-net model instead of the enhanced row-column-net model. Table 5.2 displays average performance results of sHP$_{RCN}$ and sHP$_{eRCN}$ over the three different matrix categories as well as the overall averages. As seen in the table, sHP$_{eRCN}$ performs considerably better than sHP$_{RCN}$, thus showing the validity of the cutsize definition that encapsulates the right-hand side of (4.6).

We introduce Table 5.3 to show the merits of ordering individual SpMxV operations in the mHP$_{RCN}$ method. The table displays average performance results of mHP$_{RCN}$ for the random, RB, and TSP orderings over the three different matrix categories as well as the overall averages. As seen in the table, both RB and TSP orderings lead to considerable performance improvement in the mHP$_{RCN}$ method compared to the random ordering, where the TSP ordering leads to slightly better improvement than the RB ordering. In the following tables, we display the performance results of the mHP$_{RCN}$ method that utilizes TSP ordering. The TSP implementation given in [21] is used in these experiments.

Table 5.4 displays the performance comparison of the existing and proposed methods for small-to-medium size matrices. The bottom part of the table shows the geometric means of the performance results of the methods over the three different matrix

TABLE 5.4

Simulation results (misses) for small-to-medium size test matrices (cache size = part-weight threshold = 64 KB).

	Existing methods						Proposed methods						
	Single SpMxV										Multiple SpMxVs		
	sBFS [34]		sRCM [24] Modified		sHP$_{RN}$ [41] (1D part.)		sHP$_{CN}$ (1D part.)		sHP$_{eRCN}$ (2D part.)		mHP$_{RCN}$ (2D partitioning)		
	x	$x+y$	x	$x+y$	x	$x+y$	x	$x+y$	x	$x+y$	x	y	$x+y$
Symmetric matrices													
ncvxqp9	0.51	0.59	0.52	0.60	0.37	0.48	0.28	**0.40**	0.28	**0.40**	0.31	1.19	0.47
tuma1	0.42	**0.59**	0.58	0.71	0.62	0.73	0.56	0.69	0.56	0.69	0.45	1.01	0.60
bloweybl	1.00	1.00	1.00	1.00	0.88	0.92	0.68	0.77	0.63	**0.74**	0.63	1.02	**0.74**
bloweya	1.00	1.00	1.03	1.02	1.18	1.12	0.65	0.75	0.73	0.81	0.45	1.03	**0.62**
brainpc2	0.88	0.90	0.89	0.91	1.33	1.27	1.08	1.06	0.66	0.73	0.28	1.04	**0.43**
a5esindl	1.11	1.09	0.83	0.86	0.84	0.87	1.12	1.10	0.40	0.52	0.28	1.03	**0.43**
dixmaanl	0.33	**0.50**	0.33	**0.50**	0.34	0.51	0.34	**0.50**	0.34	**0.50**	0.36	1.01	0.52
shallow_water1	1.45	1.28	1.22	1.14	1.10	1.07	0.90	0.94	0.89	0.94	0.77	1.01	**0.86**
c-65	0.90	0.91	0.96	0.97	0.61	0.67	0.38	0.47	0.35	0.44	0.24	1.37	**0.40**
finan512	1.57	1.40	1.47	1.34	0.65	0.75	0.56	**0.68**	0.55	**0.68**	0.70	1.27	0.89
copter2	0.44	0.49	0.43	0.49	0.41	0.47	0.26	**0.33**	0.26	**0.33**	0.30	2.60	0.53
msc23052	0.46	0.51	0.42	0.47	0.52	0.57	0.40	**0.46**	0.44	0.49	0.35	2.65	0.57
Square nonsymmetric matrices													
poli_large	1.12	1.08	1.12	1.08	0.86	0.91	0.62	**0.75**	0.64	0.77	0.60	1.05	0.76
powersim	1.02	1.01	0.72	0.81	0.55	0.69	0.51	**0.66**	0.51	**0.66**	0.50	1.04	0.67
memplus	0.87	0.90	1.06	1.05	1.39	1.30	0.91	0.93	0.87	0.90	0.47	1.24	**0.63**
Zhao1	0.55	0.65	0.36	**0.51**	0.72	0.79	0.48	0.60	0.49	0.60	0.60	1.64	0.84
mult_dcop_01	0.98	0.98	1.00	1.00	0.70	0.71	0.45	0.48	0.18	0.23	0.13	1.36	**0.20**
jan99jac120sc	1.20	1.15	1.30	1.22	0.92	0.94	0.51	**0.62**	0.52	0.63	0.63	1.41	0.83
circuit_4	1.52	1.39	1.83	1.62	1.45	1.34	0.94	0.95	0.87	0.91	0.41	1.16	**0.60**
ckt11752_dc_1	0.79	0.83	0.86	0.89	0.58	0.66	0.40	0.52	0.42	0.54	0.31	1.10	**0.47**
poisson3Da	0.09	0.11	0.09	0.11	0.14	0.15	0.09	**0.10**	0.09	**0.10**	0.09	6.32	0.18
bcircuit	0.60	0.67	0.58	0.66	0.32	0.44	0.26	**0.39**	0.26	**0.39**	0.27	1.10	0.42
g7jac120	0.75	0.76	0.26	0.30	0.44	0.47	0.21	**0.25**	0.23	0.28	0.18	2.51	0.31
e40r0100	0.82	0.86	0.74	0.79	0.76	0.81	0.63	**0.71**	0.66	0.73	0.54	1.94	0.84
Rectangular matrices													
lp_dfl001	0.30	0.33	0.31	0.34	0.34	0.36	0.18	0.21	0.20	0.23	0.10	2.57	**0.19**
ge	0.40	0.47	0.34	0.41	0.30	0.37	0.25	0.33	0.25	0.33	0.21	1.23	**0.32**
ex3sta1	1.75	1.47	1.14	1.09	1.23	1.14	0.86	0.91	0.81	**0.88**	0.81	1.09	0.91
lp_stocfor3	1.74	1.48	1.64	1.42	0.79	**0.86**	0.80	0.87	0.80	0.87	0.79	1.02	0.87
cq9	0.40	0.44	0.39	0.43	0.45	0.48	0.30	0.34	0.38	0.42	0.18	1.54	**0.27**
psse0	0.45	0.64	0.43	0.63	0.44	0.64	0.41	0.62	0.41	0.62	0.28	1.01	**0.53**
co9	0.43	0.47	0.38	0.42	0.46	0.50	0.34	0.39	0.41	0.46	0.18	1.54	**0.27**
baxter	0.69	0.75	0.67	0.74	0.47	0.57	0.45	0.56	0.43	0.54	0.30	1.09	**0.45**
graphics	0.74	0.87	0.80	0.91	0.68	0.84	0.48	**0.75**	0.49	**0.75**	0.55	1.01	0.79
fome12	0.29	0.31	0.32	0.35	0.32	0.35	0.18	0.21	0.19	0.22	0.10	2.74	**0.20**
route	0.34	0.36	0.48	0.50	0.37	0.39	0.62	0.64	0.59	0.61	0.08	1.38	**0.12**
fxm4_6	1.54	1.41	1.23	1.18	0.86	0.89	0.70	**0.77**	0.71	0.78	0.75	1.17	0.85
Geometric means													
Symmetric	0.74	0.80	0.73	0.79	0.67	0.74	0.54	0.64	0.47	0.58	0.40	1.26	0.57
Nonsymmetric	0.74	0.76	0.66	0.70	0.63	0.68	0.43	0.51	0.40	0.48	0.34	1.54	0.50
Rectangular	0.60	0.64	0.57	0.62	0.51	0.57	0.41	0.49	0.43	0.51	0.27	1.36	0.40
Overall	0.69	0.73	0.65	0.70	0.60	0.66	0.45	0.54	0.43	0.52	0.33	1.38	0.48

categories as well as the overall averages. Among the existing methods, sHP$_{RN}$ performs considerably better than both sBFS and sRCM for all matrix categories, on the average.

5.2.1. Comparison of 1D methods sHP$_{RN}$ and sHP$_{CN}$. Here we present the experimental comparison of sHP$_{RN}$ and sHP$_{CN}$ and show how this experimental comparison relates to the theoretical comparison given in section 4.1.1. As seen

TABLE 5.5

Sensitivity of sHP$_{RN}$[41] and sHP$_{CN}$ to cache-line size (cache size = part-weight threshold = 64 KB).

Line size (byte)	Nonsymmetric		Rectangular	
	sHP$_{RN}$	sHP$_{CN}$	sHP$_{RN}$	sHP$_{CN}$
	x	x	x	x
8	0.70	0.53	0.62	0.52
16	0.68	0.49	0.58	0.47
32	0.65	0.45	0.52	0.41
64	0.61	0.41	0.44	0.34
128	0.57	0.38	0.39	0.28
256	0.52	0.33	0.36	0.23
512	0.33	0.30	0.23	0.23

in Table 5.4, sHP$_{CN}$ performs significantly better than sHP$_{RN}$, on the overall average. sHP$_{CN}$ performs better than sHP$_{RN}$ in all of the 36 reordering instances except `a5esindl`, `lp_stocfactor3`, and `route`. The significant performance gap between sHP$_{RN}$ and sHP$_{CN}$ in favor of sHP$_{CN}$ even for symmetric matrices confirms our expectation that temporal locality is more important than spatial locality in SpMxV operations that involve irregularly sparse matrices.

We introduce Table 5.5 to experimentally investigate the sensitivity of the sHP$_{RN}$ and sHP$_{CN}$ methods to the cache-line size. In the construction of the averages reported in this table, simulation results of every method are normalized with respect to those of the original ordering with the respective cache-line size. We also utilize Table 5.5 to provide fairness in the comparison of sHP$_{RN}$ and sHP$_{CN}$ methods for nonsymmetric square and rectangular matrices. Some of the nonsymmetric square and rectangular matrices may be more suitable for rowwise partitioning by the column-net model, whereas some other matrices may be more suitable for columnwise partitioning utilizing the row-net model. This is because of the differences in row and column sparsity patterns of a given nonsymmetric or rectangular matrix. Hendrickson and Kolda [22] and Ucar and Aykanat [37] provide discussions on choosing partitioning dimension depending on the individual matrix characteristics in the parallel SpMxV context. In the construction of Table 5.5, each of the sHP$_{RN}$ and sHP$_{CN}$ methods is applied on both A and A^T matrices, and the better result is reported for the respective method on the reordering of matrix A. Here the performance of CSR-based SpMxV $y \leftarrow A^T x$ is assumed to simulate the performance of CSC-based $y \leftarrow Ax$. Comparison of the results in Table 5.5 for the line size of 64 bytes and the average results in Table 5.4 shows that the performance of both methods increases due to the selection of a better partitioning dimension (especially for rectangular matrices), while the performance gap remains almost the same.

As seen in Table 5.5, the performance of sHP$_{RN}$ is considerably more sensitive to the cache-line size than that of sHP$_{CN}$. For nonsymmetric matrices, as the line size is increased from eight bytes (one word) to 512 bytes, the average normalized cache-miss count decreases from 0.70 to 0.33 in the sHP$_{RN}$ method, whereas it decreases from 0.53 to 0.30 in the sHP$_{CN}$ method. Similarly, for rectangular matrices, the average normalized cache-miss count decreases from 0.62 to 0.23 in the sHP$_{RN}$ method, whereas it decreases from 0.52 to 0.23 in the sHP$_{CN}$ method. As seen in Table 5.5, the performance of these two methods becomes very close for the largest line size of 512 bytes (64 words). This experimental finding conforms to our expectation that sHP$_{RN}$ exploits spatial locality better than sHP$_{CN}$, whereas sHP$_{CN}$ exploits temporal locality better than sHP$_{RN}$.

5.2.2. Comparison of 1D and 2D methods. We proceed with the relative performance comparison of the 1D and 2D partitioning based methods, which will be

referred to as 1D methods and 2D methods, respectively, in the rest of the paper. As seen in Table 5.4, on the average, 2D methods sHP_{eRCN} and mHP_{RCN} perform better than 1D methods sHP_{RN} and sHP_{CN}. The performance gap between the 2D and 1D methods is considerably higher in reordering symmetric matrices in favor of 2D methods. This experimental finding may be attributed to the relatively restricted search space of the column-net model (as well as the row-net model) in 1D partitioning of symmetric matrices. The relative performance comparison of 2D methods shows that sHP_{eRCN} and mHP_{RCN} display comparable performance for symmetric matrices, whereas mHP_{RCN} performs much better than sHP_{eRCN} for nonsymmetric and rectangular matrices, on the average. mHP_{RCN} performs 8.3% better than sHP_{eRCN} in terms of cache misses due to the access of x-vector and y-vector entries, on the overall average.

As seen in Table 5.4, mHP_{RCN} incurs significantly fewer x-vector entry misses than sHP_{eRCN} on the overall average. This is expected because the multiple-SpMxV framework utilized in mHP_{RCN} enables better exploitation of temporal locality in accessing x-vector entries. However, the increase in the y-vector entry misses, which is introduced by the multiple-SpMxV framework, does not amortize in some of the reordering instances. As expected, mHP_{RCN} performs better than sHP_{eRCN} in the reordering of matrices that contain dense rows. For example, in the reordering of symmetric matrices `a5esindl`, `bloweya`, and `brainpc2`, which, respectively, contain dense rows with 9993, 10001, and 13799 nonzeros, mHP_{RCN} performs significantly better than sHP_{eRCN}. Similar experimental findings can be observed in Table 5.4 for the following matrices that contain dense rows: square nonsymmetric matrices `circuit_4`, `ckt11752_dc_1`, and `mult_dcop_01` and rectangular matrices `baxter`, `co9`, `cq9`, and `route`. Although `shallow_water` and `psse0` do not contain dense rows (the maximum number of nonzeros in a row is only four in both matrices), mHP_{RCN} performs significantly better than sHP_{eRCN} in reordering these two matrices. mHP_{RCN} incurs significantly fewer cache misses due to the access of x-vector entries while incurring a very small number of additional cache misses due to the access of y-vector entries. The reason behind the latter finding is the very small number of shared rows among the A^k matrices obtained by mHP_{RCN} in splitting these two matrices. For example, in one of the splittings generated by mHP_{RCN}, among the 81920 rows of `shallow_water`, only 785 rows are shared, and all of them are shared between only two distinct A^k matrices.

5.2.3. Experimental sensitivity analysis. Table 5.6 shows the comparison of the sensitivities of the proposed methods sHP_{CN}, sHP_{eRCN}, and mHP_{RCN} to the cache-line size. In the construction of the averages reported in this table, simulation results of every method are normalized with respect to those of the original ordering with the respective cache-line size. In terms of cache misses due to access of x-vector entries, the performance of each method compared to the original ordering increases with increasing cache-line size. However, in terms of cache misses due to access of y-vector entries, the performance of mHP_{RCN} compared to the original ordering decreases with increasing cache-line size. So, with increasing cache-line size, the performance gap between mHP_{RCN} and the other two methods sHP_{CN} and sHP_{eRCN} increases so that sHP_{eRCN} performs better than mHP_{RCN} for larger cache-line size of 512 bytes. This experimental finding can be attributed to the deficiency of the multiple-SpMxV framework in exploiting spatial locality in accessing y-vector entries. We believe that models and methods need to be investigated for intelligent global row reordering to overcome this deficiency of the multiple-SpMxV framework.

TABLE 5.6

Sensitivity of sHP_{CN}, sHP_{eRCN}, and mHP_{RCN} to cache-line size (cache size = part-weight threshold = 64 KB).

Line size (byte)	Single SpMxV				Multiple SpMxVs		
	sHP_{CN}		sHP_{eRCN}		mHP_{RCN}		
	x	$x+y$	x	$x+y$	x	y	$x+y$
8	0.59	0.69	0.59	0.69	0.47	1.09	0.62
16	0.55	0.64	0.55	0.64	0.43	1.15	0.58
32	0.50	0.59	0.49	0.59	0.36	1.23	0.52
64	0.45	0.54	0.43	0.52	0.33	1.38	0.48
128	0.41	0.49	0.38	0.46	0.28	1.50	0.43
256	0.37	0.44	0.33	0.40	0.24	1.60	0.38
512	0.36	0.42	0.30	0.36	0.25	1.83	0.38

TABLE 5.7

Sensitivity of HP-based reordering methods to the part-weight threshold (cache size = 64 KB).

Part size (KB)	1D partitioning				2D partitioning				
	sHP_{RN} [41]		sHP_{CN}		sHP_{eRCN}		mHP_{RCN}		
	x	$x+y$	x	$x+y$	x	$x+y$	x	y	$x+y$
512	0.79	0.81	0.71	0.75	0.69	0.73	0.63	1.08	0.69
256	0.68	0.72	0.61	0.67	0.57	0.63	0.49	1.15	0.58
126	0.62	0.68	0.51	0.59	0.48	0.56	0.39	1.28	0.52
64	0.60	0.66	0.45	0.54	0.43	0.52	0.34	1.42	0.50
32	0.59	0.66	0.43	0.52	0.42	0.51	0.33	1.53	0.51
16	0.60	0.66	0.43	0.52	0.42	0.51	0.34	1.57	0.52
8	0.61	0.67	0.43	0.52	0.42	0.51	0.35	1.61	0.54

We introduce Table 5.7 to display the sensitivities (as overall averages) of the HP-based reordering methods to the part-weight threshold (W_{max}) used in terminating the RB process. The performance of each method increases with decreasing part-weight threshold until the part-weight threshold becomes equal to the cache size. For each method, the rate of performance increase begins to decrease as the part-weight threshold becomes closer to the cache size. The performance of each method remains almost the same with decreasing part-weight threshold below the cache size except mHP_{RCN}. The slight decrease in the performance of mHP_{RCN} with decreasing part-weight threshold below the cache size can be attributed to the increase in the number of y misses with an increasing number of A^k matrices because of the deficiency of the multiple-SpMxV framework in exploiting spatial locality in accessing y-vector entries. These experimental findings show the validity of Theorems 4.1, 4.2, and 4.3 for the effectiveness of the proposed sHP_{CN}, sHP_{eRCN}, and mHP_{RCN} methods, respectively. Although the proposed HP-based methods are cache-size–aware methods, those that utilize the single-SpMxV framework can easily be modified to become cache-oblivious methods by continuing the RB process until the parts become sufficiently small or the qualities of the bipartitions drop below a predetermined threshold.

5.3. OSKI experiments. For large size matrices, OSKI experiments are performed by running OSKI version 1.0.1h (compiled with `gcc`) on a machine with 2.66 GHz Intel Q8400 and 4 GB of RAM, where each core pair shares 2 MB 8-way set-associative L2 cache. The generalized compressed sparse row (GCSR) format available in OSKI is used for all reordering methods. GCSR handles empty rows by augmenting the traditional CSR with an optional list of nonempty row indices, thus enabling the multiple-SpMxV framework. For each reordering instance, an SpMxV workload contains 100 calls to `oski_MatMult()` with the same matrix after three calls as a warm-up.

Table 5.8 displays the performance comparison of the existing and proposed methods for large size matrices. In the table, the first column shows OSKI runtimes

TABLE 5.8
OSKI runtimes for large size test matrices (cache size = part-weight threshold = 2 MB).

	Actual		Normalized w.r.t. actual times on original order					
	Original order		Existing methods			Proposed methods		
			Single SpMxV					Mult. SpMxVs
	not tuned (ms)	OSKI tuned	sBFS [34]	sRCM [24] modified	sHP_{RN} [41] (1D part.)	sHP_{CN} (1D part.)	sHP_{eRCN} (2D part.)	mHP_{RCN} (2D part.)
				Symmetric matrices				
c-73	0.454	1.00	1.02	1.06	0.93	0.92	0.92	**0.90**
c-73b	0.456	1.00	1.01	1.07	0.93	0.92	0.91	**0.89**
rgg_n_2_17_s0	0.503	0.95	0.92	1.07	0.89	0.82	**0.76**	0.91
boyd2	0.726	1.19	1.00	1.14	0.95	0.92	0.89	**0.85**
ins2	1.207	1.00	0.96	2.32	0.97	1.06	0.97	**0.67**
rgg_n_2_18_s0	1.051	0.96	0.90	1.07	0.99	0.99	**0.75**	0.81
				Square nonsymmetric matrices				
Raj1	0.629	1.04	0.88	0.96	0.86	**0.82**	0.83	0.84
rajat21	0.953	1.07	1.01	1.16	1.00	0.95	0.96	**0.90**
rajat24	0.963	1.02	1.04	1.16	0.99	0.94	0.96	**0.91**
ASIC_320k	1.436	0.99	1.09	1.44	0.97	0.92	0.73	**0.64**
Stanford_Berkeley	2.325	1.04	1.01	1.05	1.10	1.01	**0.89**	0.98
				Rectangular matrices				
kneser_10_4_1	0.694	1.02	0.70	0.87	0.81	**0.67**	0.89	0.68
neos	0.697	1.26	1.14	1.19	1.00	**0.95**	**0.95**	0.96
wheel_601	1.377	1.27	0.82	0.75	0.69	0.69	0.66	**0.52**
LargeRegFile	2.643	1.55	1.19	1.30	1.04	**0.95**	**0.95**	0.96
cont1_l	2.939	1.14	1.04	1.19	1.05	**0.93**	**0.93**	0.95
degme	2.770	1.04	0.77	1.26	0.87	0.77	0.78	**0.74**
				Geometric means				
Symmetric	-	1.01	0.97	1.23	0.94	0.94	0.86	0.84
Nonsymmetric	-	1.03	1.00	1.14	0.98	0.93	0.87	0.84
Rectangular	-	1.20	0.93	1.07	0.90	0.82	0.85	0.78
Overall	-	1.08	0.96	1.15	0.94	0.89	0.86	0.82

without tuning for original matrices. The second column shows the normalized OSKI runtimes obtained through the full tuning enforced by the ALWAYS_TUNE_AGGRESSIVELY parameter for original matrices. The other columns show the normalized runtimes obtained through the reordering methods. Each normalized value is calculated by dividing the OSKI time of the respective method by the untuned OSKI runtime for the original matrices. As seen in the first two columns of the table, optimizations provided through the OSKI package do not improve the performance of the SpMxV operation performed on the original matrices. This experimental finding can be attributed to the irregularly sparse nature of the test matrices. We should mention that optimizations provided through the OSKI package do not improve the performance of the SpMxV operation performed on the reordered matrices.

The relative performance figures given in Table 5.8 for different reordering methods in terms of OSKI times in general conform to the relative performance discussions given in section 5.2 based on the cache-miss simulation results. As seen in Table 5.8, on the overall average, the 2D methods sHP_{eRCN} and mHP_{RCN} perform better than the 1D methods sHP_{RN} and sHP_{CN}, where mHP_{RCN} (adopting the multiple-SpMxV framework) is the clear winner. Furthermore, for the relative performance comparison of the 1D methods, the proposed sHP_{CN} method performs better than the existing sHP_{RN} method. On the overall average, sHP_{CN}, sHP_{eRCN}, and mHP_{RCN} achieve significant speedup by reducing the SpMxV times by 11%, 14%, and 18%, respectively, compared to the unordered matrices, thus confirming the success of the proposed reordering methods.

Table 5.9 shows cache-miss simulation results for large size matrices, and it is introduced to show how the performance comparison in terms of cache-miss simulations relates to performance comparison in terms of OSKI runtimes. In Table 5.9, the *tot* column shows the normalized total number of cache misses including compulsory

TABLE 5.9

Simulation results (misses) for large size test matrices (cache size = part-weight threshold = 2 MB).

	Existing methods						Proposed methods					
	Single SpMxV										M. SpMxVs		
	sBFS [34]		sRCM [24] modified		sHP$_{RN}$ [41] (1D part.)		sHP$_{CN}$ (1D part.)		sHP$_{eRCN}$ (2D part.)		mHP$_{RCN}$ (2D part.)	
	$x+y$	tot	$x+y$	tot	$x+y$	tot	$x+y$	tot	$x+y$	tot	$x+y$	tot
Symmetric matrices												
c-73	0.99	1.00	1.00	1.00	0.69	0.94	0.59	0.92	0.60	0.92	**0.53**	0.91
c-73b	0.99	1.00	1.00	1.00	0.69	0.94	0.59	0.92	0.60	0.92	**0.53**	0.91
rgg_n_2_17_s0	**0.97**	1.00	1.02	1.00	1.10	1.01	1.14	1.01	1.02	1.00	0.98	1.00
boyd2	1.02	1.01	1.09	1.14	0.83	0.94	0.72	0.91	0.68	0.90	**0.55**	0.85
ins2	0.94	0.98	1.31	1.18	0.94	0.98	0.94	0.98	0.89	0.96	**0.19**	0.71
rgg_n_2_18_s0	**0.98**	1.00	1.01	1.00	1.69	1.05	1.58	1.04	1.05	1.00	1.00	1.00
Square nonsymmetric matrices												
Raj1	0.98	0.99	0.96	0.99	0.73	0.94	0.62	0.91	0.66	0.92	**0.58**	0.90
rajat21	1.36	1.08	1.37	1.08	1.15	1.03	0.88	0.97	0.98	1.00	**0.75**	0.95
rajat24	1.53	1.11	1.46	1.09	1.09	1.02	0.81	0.96	0.96	0.99	**0.67**	0.93
ASIC_320k	1.61	1.17	1.61	1.16	0.89	0.97	0.79	0.94	0.57	0.88	**0.32**	0.82
Stanford_Berkeley	1.20	1.02	1.65	1.07	1.48	1.04	0.94	0.99	1.07	1.01	**0.71**	0.97
Rectangular matrices												
kneser_10_4_1	1.33	1.09	1.50	1.13	1.18	1.05	**0.85**	0.96	1.14	1.04	**0.85**	0.97
neos	1.12	1.03	1.13	1.03	1.00	1.00	**0.92**	0.98	**0.92**	0.98	**0.92**	0.98
wheel_601	1.39	1.10	1.40	1.10	1.16	1.04	1.02	1.00	1.14	1.03	**0.91**	0.98
LargeRegFile	1.99	1.20	1.89	1.18	1.56	1.11	**1.00**	1.00	**1.00**	1.00	**1.00**	1.00
cont1_l	1.25	1.06	1.27	1.07	1.01	1.00	**0.75**	0.94	**0.75**	0.94	0.76	0.94
degme	0.35	0.86	1.06	1.01	0.68	0.93	0.36	0.86	0.43	0.88	**0.21**	0.83
Geometric means												
Symmetric	0.98	1.00	1.07	1.05	0.94	0.98	0.87	0.96	0.78	0.95	0.55	0.89
Nonsymmetric	1.32	1.07	1.38	1.08	1.04	1.00	0.80	0.96	0.82	0.96	0.58	0.91
Rectangular	1.10	1.05	1.35	1.09	1.06	1.02	0.77	0.96	0.85	0.98	0.69	0.95
Overall	1.12	1.04	1.25	1.07	1.01	1.00	0.81	0.96	0.82	0.96	0.61	0.92

TABLE 5.10

Average normalized reordering overhead and average number of SpMxV operations required to amortize the reordering overhead.

	Existing methods				Proposed methods					
	Single SpMxV								Multiple SpMxVs	
	sBFS [34]		sHP$_{RN}$ [41] (1D part.)		sHP$_{CN}$ (1D part.)		sHP$_{eRCN}$ (2D part.)		mHP$_{RCN}$ (2D partitioning)	
	Over-head	Amor-tization	Over-head	Amor-tization	Over-head	Amor-tization	Over-head	Amor-tization	Over-head	Amor-tization
Symmetric	17	465	194	3135	190	1716	514	3732	920	5097
Nonsymmetric	26	700	314	5078	304	2740	664	4822	1198	6640
Rectangular	23	621	383	6197	254	2292	620	4503	1240	6870
Overall	22	587	286	4620	245	2209	596	4327	1110	6149

cache misses due to the access of matrix nonzeros. The total numbers of cache misses are also displayed since these values actually determine the performance of the reordering methods in terms of OSKI times. Comparison of Tables 5.8 and 5.9 shows that the amount of performance improvement attained by the proposed methods in terms of OSKI times is in general considerably higher than the amount of performance improvement in terms of the total number of cache misses. For example, sHP$_{eRCN}$ performs only 4% fewer cache misses than the unordered case, whereas it achieves 14% less OSKI runtime, on the overall average.

Table 5.10 is introduced to evaluate the preprocessing overhead of the reordering methods. For each test matrix, the reordering times of all methods are normalized with respect to the OSKI time of the SpMxV operation using the unordered matrix,

and the geometric averages of these normalized values are displayed in the "over-head" column of the table. In the table, the "amortization" column denotes the average number of SpMxV operations required to amortize the reordering overhead. Each "amortization value" is obtained by dividing the average normalized reordering overhead by the overall average OSKI time improvement taken from Table 5.8. Overhead and amortization values are not given for the sRCM method since sRCM does not improve the OSKI runtime at all.

As seen in Table 5.10, top-down HP-based methods are significantly slower than the bottom-up sBFS method. The runtimes of the two 1D methods sHP_{RN} and sHP_{CN} are comparable, as expected. As also seen in the table, the 2D methods are considerably slower than the 1D methods, as expected. In the column-net hypergraph model used in the 1D method sHP_{CN}, the number of vertices and the number of nets are equal to the number of rows and the number of columns, respectively, and the number of pins is equal to the number of nonzeros. In the hypergraph model used in the 2D methods, the number of vertices and the number of nets are equal to the number of nonzeros and the number of rows plus the number of columns, respectively, and the number of pins is equal to two times the number of nonzeros. That is, the hypergraphs used in the 2D methods are considerably larger than the hypergraphs used in the 1D methods. So partitioning the hypergraphs used in the 2D methods takes a considerably longer time than partitioning the hypergraphs used in the 1D methods, and the runtime difference becomes higher with increasing matrix density in favor of the 1D methods. There exists a considerable difference in the runtimes of the two 2D methods sHP_{eRCN} and mHP_{RCN} in favor of sHP_{eRCN}. This is because of the removal of the vertices connected by the cut row nets in the enhanced row-column-net model used in sHP_{eRCN}.

As seen in Table 5.10, the top-down HP methods amortize for a larger number of SpMxV computations compared to the bottom-up sBFS method. For example, the use of sHP_{CN} instead of sBFS amortizes after 276% more SpMxV computations on the overall average. As also seen in the table, the 2D methods amortize for a larger number of SpMxV computations compared to the 1D methods. For example, the use of mHP_{RCN} instead of sHP_{CN} amortizes after 178% more SpMxV computations.

6. Conclusion. Single- and multiple-SpMxV frameworks were investigated for exploiting cache locality in SpMxV computations that involve irregularly sparse matrices. For the single-SpMxV framework, two cache-size–aware top-down row/column-reordering methods based on 1D and 2D sparse matrix partitioning were proposed by utilizing the column-net and enhancing the row-column-net hypergraph models of sparse matrices. The multiple-SpMxV framework requires splitting a given matrix into a sum of multiple nonzero-disjoint matrices so that the SpMxV operation is computed as a sequence of multiple input- and output-dependent SpMxV operations. For this framework, a cache-size–aware top-down matrix splitting method based on 2D matrix partitioning was proposed by utilizing the row-column-net hypergraph model of sparse matrices. The proposed hypergraph partitioning (HP) based methods in the single-SpMxV framework primarily aim at exploiting temporal locality in accessing input-vector entries, and the proposed HP-based method in the multiple-SpMxV framework aims at exploiting temporal locality in accessing both input- and output-vector entries.

The performances of the proposed models and methods were evaluated on a wide range of sparse matrices. The experiments were carried out in two different settings: cache-miss simulations and actual runs using OSKI. Experimental results showed that

the proposed methods and models outperform the state-of-the-art schemes, and these results also conformed to our expectation that temporal locality is more important than spatial locality (for practical line sizes) in SpMxV operations that involve irregularly sparse matrices. The two proposed methods that are based on 2D matrix partitioning were found to perform better than the proposed method based on 1D partitioning at the expense of higher reordering overhead, where the 2D method within the multiple-SpMxV framework was the clear winner.

REFERENCES

[1] R. C. AGARWAL, F. G. GUSTAVSON, AND M. ZUBAIR, *A high performance algorithm using pre-processing for the sparse matrix-vector multiplication*, in Proceedings of Supercomputing '92 (Minneapolis, MN), IEEE, Washington, DC, 1992, pp. 32–41.

[2] K. AKBUDAK, E. KAYASLAN, AND C. AYKANAT, *Hypergraph-Partitioning-Based Models and Methods for Exploiting Cache Locality in Sparse-Matrix Vector Multiplication*, Technical report BU-CE-1201, Computer Engineering Department, Bilkent University, Ankara, Turkey, 2012; also available online at http://www.cs.bilkent.edu.tr/tech-reports/2012/BU-CE-1201.pdf.

[3] I. AL-FURAIH AND S. RANKA, *Memory hierarchy management for iterative graph structures*, in IPPS/SPDP, IEEE, Washington, DC, 1998, pp. 298–302.

[4] C. AYKANAT, A. PINAR, AND Ü. V. ÇATALYÜREK, *Permuting sparse rectangular matrices into block-diagonal form*, SIAM J. Sci. Comput., 25 (2004), pp. 1860–1879.

[5] Z. BAI, J. DEMMEL, J. DONGARRA, A. RUHE, AND H. VAN DER VORST, *Templates for the Solution of Algebraic Eigenvalue Problems: A Practical Guide*, SIAM, Philadelphia, 2000.

[6] M. W. BERRY, B. HENDRICKSON, AND P. RAGHAVAN, *Sparse matrix reordering schemes for browsing hypertext*, in The Mathematics of Numerical Analysis, Lectures Appl. Math. 32, AMS, Providence, RI, 1996, pp. 99–123.

[7] Ü. V. ÇATALYÜREK AND C. AYKANAT, *Decomposing irregularly sparse matrices for parallel matrix-vector multiplications*, in Proceedings of the 3rd International Symposium on Solving Irregularly Structured Problems in Parallel, Irregular '96, Lecture Notes in Comput. Sci. 1117, Springer-Verlag, Berlin, 1996, pp. 75–86.

[8] Ü. V. ÇATALYÜREK AND C. AYKANAT, *Hypergraph-partitioning based decomposition for parallel sparse-matrix vector multiplication*, IEEE Trans. Parallel Distributed Systems, 10 (1999), pp. 673–693.

[9] Ü. V. ÇATALYÜREK AND C. AYKANAT, *PaToH: A Multilevel Hypergraph Partitioning Tool, Version* 3.0, Department of Computer Engineering, Bilkent University, Ankara, Turkey; available online at http://bmi.osu.edu/∼umit/software.htm, 1999.

[10] Ü. V. ÇATALYÜREK AND C. AYKANAT, *A fine-grain hypergraph model for* 2D *decomposition of sparse matrices*, in Proceedings of the 15th International Parallel and Distributed Processing Symposium, IEEE, Washington, DC, p. 118.

[11] Ü. V. ÇATALYÜREK, C. AYKANAT, AND B. UÇAR, *On two-dimensional sparse matrix partitioning: Models, methods, and a recipe*, SIAM J. Sci. Comput., 32 (2010), pp. 656–683.

[12] J. M. CRUMMEY, D. WHALLEY, AND K. KENNEDY, *Improving memory hierarchy performance for irregular applications using data and computation reorderings*, Internat. J. Parallel Programming, 29 (2001), pp. 217–247.

[13] R. DAS, D. J. MAVRIPLIS, J. SALTZ, S. GUPTA, AND R. PONNUSAMY, *The design and implementation of a parallel unstructured Euler solver using software primitives*, AIAA J., 1992 (1992), AIAA-92-0562.

[14] T. A. DAVIS AND Y. HU, *The University of Florida sparse matrix collection*, ACM Trans. Math. Software, 38 (2011), p. 1.

[15] C. DING AND K. KENNEDY, *Improving cache performance in dynamic applications through data and computation reorganization at run time*, SIGPLAN Not., 34 (1999), pp. 229–241.

[16] E. ELMROTH, F. GUSTAVSON, I. JONSSON, AND B. KÅGSTRÖM, *Recursive blocked algorithms and hybrid data structures for dense matrix library software*, SIAM Rev., 46 (2004), pp. 3–45.

[17] J. D. FRENS AND D. S. WISE, *Auto-blocking matrix-multiplication or tracking blas3 performance from source code*, SIGPLAN Not., 32 (1997), pp. 206–216.

[18] G. HAASE, M. LIEBMANN, AND G. PLANK, *A Hilbert-order multiplication scheme for unstructured sparse matrices*, Int. J. Parallel Emerg. Distrib. Syst., 22 (2007), pp. 213–220.

[19] H. HAN AND C. TSENG, *Exploiting locality for irregular scientific codes*, IEEE Trans. Parallel Distributed Systems, 17 (2006), pp. 606–618.

[20] S. A. HAQUE AND S. HOSSAIN, *A note on the performance of sparse matrix-vector multiplication with column reordering*, in Proceedings of the International Conference on Computing, Engineering and Information, IEEE, Washington, DC, 2009, pp. 23–26.

[21] K. HELSGAUN, *An effective implementation of the Lin-Kernighan traveling salesman heuristic*, European J. Oper. Res., 126 (2000), pp. 106–130.

[22] B. HENDRICKSON AND T. G. KOLDA, *Partitioning rectangular and structurally nonsymmetric sparse matrices for parallel processing*, SIAM J. Sci. Comput., 21 (2000), pp. 2048–2072.

[23] D. B. HERAS, V. B. PÉREZ, J. C. CABALEIRO, AND F. F. RIVERA, *Modeling and improving locality for the sparse-matrix-vector product on cache memories*, Future Generation Comp. Syst., 18 (2001), pp. 55–67.

[24] E. IM AND K. YELICK, *Optimizing Sparse Matrix Vector Multiplication on SMPs*, in 9th SIAM Conference on Parallel Processing for Scientific Computing, SIAM, Philadelphia, 1999.

[25] G. JIN AND M. J. CRUMMEY, *Using space-filling curves for computation reordering*, in Proceedings of the Los Alamos Computer Science Institute Sixth Annual Symposium (published on CD), Los Alamos National Labs, Sante Fe, NM, 2005.

[26] G. KARYPIS, V. KUMAR, R. AGGARWAL, AND S. SHEKHAR, *hMeTiS: A Hypergraph Partitioning Package Version* 1.0.1, Department of Computer Science and Engineering, Army HPC Research Center, University of Minnesota, Minneapolis, MN, 1998.

[27] J. KOSTER, *Parallel Templates for Numerical Linear Algebra, a High-Performance Computation Library*, Master's thesis, Utrecht University, Utrecht, The Netherlands, 2002.

[28] T. LENGAUER, *Combinatorial Algorithms for Integrated Circuit Layout*, Wiley–Teubner, Chichester, UK, 1990.

[29] R. MIRCHANDANEY, J. H. SALTZ, R. M. SMITH, D. M. NICO, AND K. CROWLEY, *Principles of runtime support for parallel processors*, in Proceedings of the 2nd International Conference on Supercomputing, ICS '88, ACM, New York, 1988, pp. 140–152.

[30] J. C. PICHEL, D. B. HERAS, J. C. CABALEIRO, AND F. F. RIVERA, *Increasing data reuse of sparse algebra codes on simultaneous multithreading architectures*, Concurrency Comput. Practice Experience, 21 (2009), pp. 1838–1856.

[31] J. C. PICHEL, D. B. HERAS, J. C. CABALEIRO, AND F. F. RIVERA, *Performance optimization of irregular codes based on the combination of reordering and blocking techniques*, Parallel Comput., 31 (2005), pp. 858–876.

[32] A. PINAR AND M. T. HEATH, *Improving performance of sparse matrix-vector multiplication*, in Proceedings of the 1999 ACM/IEEE Conference on Supercomputing (CDROM), Supercomputing '99, ACM, New York, 1999, p. 30.

[33] Y. SAAD, *Iterative Methods for Sparse Linear Systems*, 2nd ed., SIAM, Philadelphia, 2003.

[34] M. M. STROUT AND P. D. HOVLAND, *Metrics and models for reordering transformations*, in Proceedings of the 2nd ACM SIGPLAN Workshop on Memory System Performance (MSP04) (Washington, DC), ACM, New York, 2004, pp. 23–34.

[35] O. TEMAM AND W. JALBY, *Characterizing the behavior of sparse algorithms on caches*, in Proceedings of Supercomputing '92 (Minneapolis, MN), IEEE, Washington, DC, 1992, pp. 578–587.

[36] S. TOLEDO, *Improving memory-system performance of sparse matrix-vector multiplication*, IBM J. Research Development, 41 (1997), pp. 711–725.

[37] B. UCAR AND C. AYKANAT, *Partitioning sparse matrices for parallel preconditioned iterative methods*, SIAM J. Sci. Comput., 29 (2007), pp. 1683–1709.

[38] B. VASTENHOUW AND R. H. BISSELING, *A two-dimensional data distribution method for parallel sparse matrix-vector multiplication*, SIAM Rev., 47 (2005), pp. 67–95.

[39] R. VUDUC, J. W. DEMMEL, AND K. A. YELICK, *OSKI: A library of automatically tuned sparse matrix kernels*, J. Phys. Conference Series, 16 (2005), p. 521.

[40] J. WHITE AND P. SADAYAPPAN, *On improving the performance of sparse matrix-vector multiplication*, in Proceedings of the International Conference on High-Performance Computing, IEEE Computer Society, Los Alamitos, CA, 1997, pp. 578–587.

[41] A. N. YZELMAN AND R. H. BISSELING, *Cache-oblivious sparse matrix–vector multiplication by using sparse matrix partitioning methods*, SIAM J. Sci. Comput., 31 (2009), pp. 3128–3154.